Preliminary Study on sCO_2 Leakage in Helical Heat Exchanger for PWR-sCO_2 Power Cycle

Gihyeon Kim [a], Sungwook Choi [a], Jeong Ik Lee[a*]
[a]Dept. Nuclear & Quantum Eng., KAIST, 373-1, Guseong-dong, Yuseong-gu, Daejeon, 305-701, Republic of Korea
[*]Corresponding author: jeongiklee@kaist.ac.kr

***Keywords :** sCO_2 Brayton cycle, Helical heat exchanger, CO_2 rupture accident

1. Introduction

The International Maritime Organization (IMO) greenhouse gas strategy aims to reduce the carbon intensity of international shipping, making the replacement of diesel engines in container ships inevitable [1]. Nuclear-based marine propulsion strategies are gaining attention as a key candidate for ship decarbonization. Marine nuclear propulsion systems have already been applied in the military sector and are now entering the civilian sector. Several countries are researching small modular reactors (SMR) for maritime operations. Having high compactness and high efficiency are required not only in the reactor core but also in the power conversion system for on-board propulsion system. In the case of KLT-40s, an actual deployment example, the power conversion system is similar in size to the reactor itself [2]. Since there are limits to reducing reactor size, minimizing the size of the power conversion system contributes to minimizing the entire propulsion system. Therefore, it would be advantageous to base the system on the well-researched pressurized water reactor (PWR) type SMR and attach a power conversion system smaller than a steam Rankine cycle.

From the perspective of compact power conversion systems, the supercritical CO_2 (sCO_2) Brayton cycle is a favored choice. Compression near the critical point enables smaller compressors, and using a high-density fluid reduces the fluid's volumetric flow rate, allowing for a smaller turbine. It also achieves high efficiency with a simple layout [3]. Therefore, selecting the sCO_2 Brayton cycle as the power conversion system is worth considering reducing the size of PWR-based SMR systems. A related issue is that the low temperature of the PWR necessitates increasing the maximum pressure of the sCO_2 cycle to boost its efficiency. This maximum pressure could potentially exceed the pressure on the PWR primary side. Consequently, if a rupture occurs in the heat exchanger between the primary and secondary sides, high-pressure CO_2 from the secondary side could leak into the primary water. From a safety analysis perspective, it is necessary to analyze the phenomena occurring in primary-secondary boundary rupture accidents to apply the sCO_2 cycle to PWR systems.

This study optimized the sCO_2 Brayton cycle based on the BANDI-60s, a PWR-based marine SMR proposed in the Republic of Korea. Based on the cycle design data, a water-sCO_2 helical heat exchanger was designed. A preliminary analysis was conducted considering the solubility of CO_2 in water in the event of a breakage accident inside the helical heat exchanger.

2. Methods and Results

2.1 sCO_2 Bryton Cycle Design

Design conditions were derived from BANDI-60s data and constraints reported for marine sCO_2 propulsion systems [4]. A simple recuperated sCO_2 layout, shown in Figure 1, was selected to prioritize compactness and meet component efficiency and minimum temperature limits.

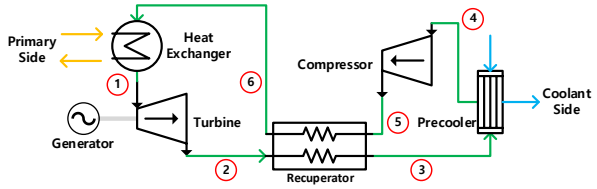

Fig. 1. Simple recuperated sCO_2 cycle

The system was designed using an in-house code KAIST-CCD. The design results that maximize cycle efficiency are summarized in Table 2. Due to the pinch point problem with the cycle design condition, the recuperator effectiveness decreased to 88.5%.

Table 1. Design parameters of sCO_2 cycle [4], [5], [6]

Parameter	Value
Thermal power (MWth)	200
Maximum pressure (MPa)	25.0
Minimum allowable pressure (MPa)	7.5
Maximum temperature (°C)	305.0
Minimum temperature (°C)	35.0
Turbine efficiency (%)	93.0
Compressor efficiency (%)	84.0
Maximum recuperator effectiveness (%)	95.0
Recuperator pressure drop (kPa)	150
Heat exchanger pressure drop (kPa)	150
Precooler pressure drop (kPa)	150

Table 2. sCO_2 cycle optimization results

Design parameter	Optimization Results
Cycle Efficiency (%)	30.1
Recuperator Effectiveness (%)	88.5
Minimum Pressure (MPa)	13.43

Mass Flow Rate (kg/sec)	1623.3
Compressor Pressure Ratio	1.88

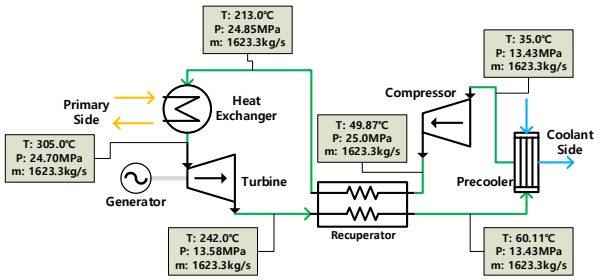

Fig. 2. Simple recuperated sCO_2 cycle

2.2 Helical Heat Exchanger Design Results

Based on the cycle design results in Figure 2, the water-sCO_2 heat exchanger design was conducted. Following the heat exchanger design of the BANDI-60s, a single helical heat exchanger concept was adopted [4]. Both the PWR primary side and the sCO_2 cycle were assumed to involve single-phase heat transfer and pressure drop. To account for pressure boundaries and reduce the mass of the spiral heat exchanger, CO_2 was assumed to flow inside the helical tube. The heat transfer coefficient was calculated using equation (1), a correlation obtained by heating the sCO_2 in a vertical helical tube [7].

$$\mathrm{Nu} = 0.019\mathrm{De}^{*1.01}\mathrm{Pr}^{0.71}\left(\frac{\rho_w}{\rho_b}\right)^{0.88}\left(\frac{\bar{c_p}}{c_{p,b}}\right)^{0.76}\left[1 + 2.2\times10^{-4}\mathrm{Ri}^{*3.56}\right]^{0.06} \cdots (1)$$

Additionally, both water and CO_2 properties calculation utilizes the REFPROP library. Table 3 lists the helical heat exchanger design conditions.

Table 3. Water-sCO_2 helical heat exchanger design conditions

Parameter	Value
Primary temperature (°C)	325 – 290
Secondary temperature (°C)	213 – 305
Primary pressure (MPa)	15.0
Secondary pressure (MPa)	24.85
Primary mass flow rate (kg/sec)	1050
Secondary mass flow rate (kg/sec)	1623.3

Table 4 presents the design results for the water-sCO_2 helical heat exchanger based on the design conditions in Table 3. Figures 3 and 4 show the heat transfer coefficients and temperatures for the primary side (water) and secondary side (CO_2), respectively. In Figure 2, the heat transfer coefficient on the secondary side ranges widely from approximately 2.8 kW/m²·K to 4 kW/m²·K. This variation is due to differences between layers, with the heat transfer coefficient decreasing toward the outer layers. For the shell side of the heat exchanger, a 2:1 ellipsoidal head was added at the top and bottom to enhance pressure resistance.

Table 4. Water-sCO_2 helical heat exchanger design results

Design parameter	Results
Primary side inner diameter (m)	3.05
Primary side outer diameter (m)	6.0
Primary side height (m)	3.0
Primary side outlet average temperature (°C)	290.0
Secondary side pipe number	5100
Secondary side layer number	60
Secondary side elevation angle (°)	6.3 - 7.4
Secondary side pressure drops (kPa)	109.1
Secondary side outlet average temperature (°C)	305.1

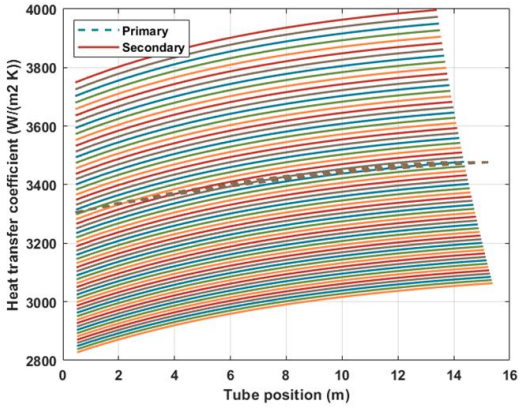

Fig. 3. Heat transfer coefficient of primary and secondary side of helical heat exchanger

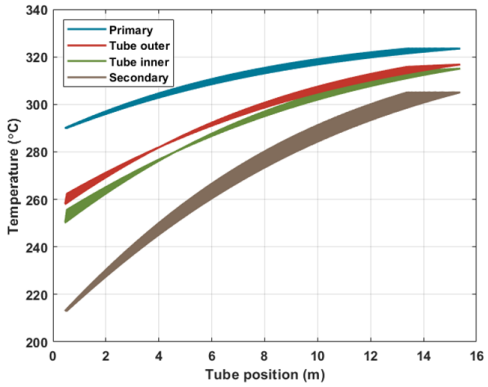

Fig. 4. Temperature of primary and secondary side of helical heat exchanger

2.3 Leakage Analysis

The shell side of the heat exchanger is the primary side. Therefore, if CO_2 leaks inside the heat exchanger, the internal pressure remains at 15 MPa while water is displaced by the CO_2. CO_2 leaked into the primary side of the reactor vessel dissolves partially in water and partially displaces water from the shell. Figure 5 illustrates this process.

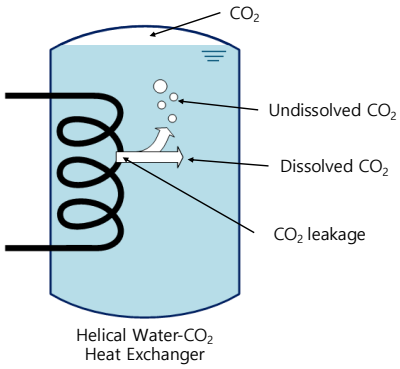

Fig. 5. Schematic of leakage process

The change in water level inside the shell over time was analyzed in the event of leakage. Based on the heat exchanger design results, conservative assumptions were applied. The rupture of the tube with the highest flow rate was assumed, and the water temperature was fixed at 325°C to represent the most unfavorable solubility conditions. The leakage flow rate was calculated without considering the choking effect.

CO_2 dissolves up to its solubility limit, and any excess CO_2 remains undissolved and displaces shell side water. Therefore, evaluating how much CO_2 dissolves in water is crucial. Using the existing Mao model, the CO_2 solubility in water was calculated for given temperature and pressure conditions [8]. Furthermore, since not all leaked CO_2 dissolves in water, the ratio of dissolved to undissolved CO_2 was incorporated into the analysis.

The displaced water volume was calculated using the ideal gas law based on the volume of CO_2 that did not dissolve in water. It was assumed that CO_2 dissolved in water at a certain dissolved rate until the solubility limit was reached, with the remaining CO_2 displacing water from the upper layer. Once the solubility limit was reached, it was interpreted that all CO_2 released displaced water from the upper layer.

Figures 6 and 7 show the displacement volume and the amount of CO_2 dissolved in water over time for different dissolved rates. The 5.88 m³ volume corresponding to a 10% reduction in water level (i.e., 90% of the normal level), based on the shell-side design criteria for the heat exchanger, is indicated by a black dashed line in Figure 6.

Compared to when the dissolved rate is 0, meaning no CO_2 is dissolved in water, the time required to displace the water increases as CO_2 dissolves more. Furthermore, once the water inside the heat exchanger becomes saturated solution, the displacement volume increases regardless of the CO_2 dissolved rate. At the given temperature, pressure, and water volume, a total of 669.5 kg of CO_2 can be dissolved in water. When all the CO_2 dissolves in the water, a flow rate equivalent to 35 minutes can be dissolved. The practical dissolution ratio (i.e., dissolved mass to total mass of released CO_2) can be obtained by referencing Lee's experimental results, which indicated that 40% of the CO_2 dissolves in water during leakage [9], [10]. The green lines in Figures 6 and 7 represent cases reflecting Lee's dissolution rate. In this case, the water level reaches 90% of the normal level (black dashed line) at 68.1 minutes due to undissolved CO_2 before the water becomes a saturated solution.

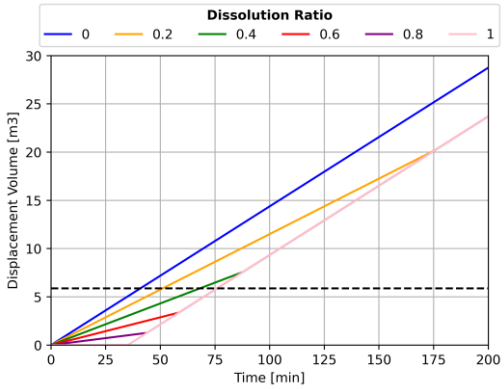

Fig. 6. Water displacement volume by leaked CO_2

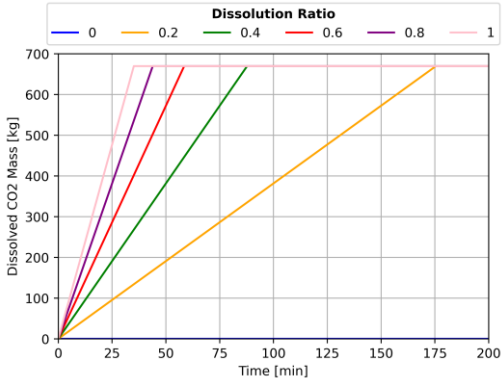

Fig.7. Dissolved mass of CO_2 during leakage

3. Summary and Conclusions

This study presented an sCO_2 Brayton cycle design for the integration with BANDI-60s to demonstrate the concept of a PWR coupled with a compact sCO_2 power cycle for ship propulsion application. The water level change on the shell side was further evaluated during a hypothetical rupture accident based on the designed helical heat exchanger, considering the CO_2 dissolution rate in high pressure high temperature water. It was confirmed that the decrease in water level is delayed as CO_2 dissolves more in water, and that the rate of water level change varies depending on the amount of CO_2 dissolved in water before the solution becomes completely saturated. Based on the existing previous experimental results, the water level was confirmed to drop to the critical level (i.e., 90% of the normal level) after 68.1 minutes.

However, applying these results directly is limited due to overly conservative assumptions for the analysis. Therefore, to better analyze the phenomena occurring on the heat exchanger shell side during CO_2 leakage into the water, it is necessary to accurately predict the CO_2 dissolution kinetic rate in water with less uncertain experiments than conducted in the past.

Therefore, future research should address the following issues. First, the critical flow rate must be

determined under conditions where CO_2 is released into high-pressure water. This will enable the determination of the maximum initial flow rate at the CO_2–water pressure boundary. Additionally, the solubility ratio and dissolution rate will be calculated under more realistic conditions. As demonstrated in this study, the transient response varies depending on the solubility ratio; therefore, accurate prediction of the solubility ratio is essential for precise accident scenario analysis. Finally, while this study analyzed only the heat exchanger, in PWRs, pumped CO_2 dissolved in water can migrate to the core; therefore, an analysis of this phenomenon will be further necessary to evaluate reactivity feedback due to the CO_2 ingress.

ACKNOWLEDGEMENTS

"This work was supported by the National Research Foundation of Korea(NRF) grant funded by the Korea government(MSIT) (No. RS-2025-25454059)."

REFERENCES

[1] T.-H. Joung, S.-G. Kang, J.-K. Lee, and J. Ahn, "The IMO initial strategy for reducing Greenhouse Gas (GHG) emissions, and its follow-up actions towards 2050," *Journal of International Maritime Safety, Environmental Affairs, and Shipping*, vol. 4, no. 1, pp. 1–7, 2020.

[2] O. Reistad and P. L. Ølgaard, "Russian Nuclear Power Plants for Marine Applications," 2006. [Online]. Available: www.nks.org

[3] Y. Ahn *et al.*, "Review of supercritical CO2 power cycle technology and current status of research and development," *Nuclear engineering and technology*, vol. 47, no. 6, pp. 647–661, 2015.

[4] IAEA, "SMALL MODULAR REACTOR TECHNOLOGY CATALOGUE," Oct. 2024.

[5] S. Son and J. I. Lee, "Application of adjoint sensitivity analysis method to supercritical CO2 power cycle optimization," *Energy*, vol. 147, pp. 1153–1164, 2018.

[6] B. S. Oh, Y. Kim, S. J. Kim, and J. I. Lee, "SMART with Trans-Critical CO2 power conversion system for maritime propulsion in Northern Sea Route, part 1: System design," *Ann. Nucl. Energy*, vol. 149, p. 107792, 2020.

[7] S. Zhang, X. Xu, C. Liu, X. Liu, Z. Ru, and C. Dang, "Experimental and numerical comparison of the heat transfer behaviors and buoyancy effects of supercritical CO2 in various heating tubes," *Int. J. Heat Mass Transf.*, vol. 149, p. 119074, 2020.

[8] S. Mao, D. Zhang, Y. Li, and N. Liu, "An improved model for calculating CO2 solubility in aqueous NaCl solutions and the application to CO2–H2O–NaCl fluid inclusions," *Chem. Geol.*, vol. 347, pp. 43–58, 2013.

[9] J. J. Lee and J. I. Lee, "Experimental Facility for Supercritical CO2 Leakage to High Pressure Water," in *Transactions of the Korean Nuclear Society Autumn Meeting*, 2020, pp. 13–14.

[10] J. J. Lee and J. I. Lee, "Preliminary Study on S-CO2 Leakage to High Pressure Water," in *Transactions of the Korean Nuclear Society Spring Meeting*, 2020.